

CFD modeling of the paraglider airfoils

Robert Kulhánek*¹

¹ ČVUT v Praze, Fakulta strojní, Ústav letadlové techniky, Technická 4, 166 07 Praha 6, Česká republika

Abstract

Paraglider is a flexible wing made from fabric material. The wing with other necessary equipment can be used for cross country flying. Advantage of a paraglider wing is its simplicity. It can be packed to a relative small backpack and has almost no requirements for landing place. Paragliding sport is very young discipline thus the paraglider designers has very limited information about aerodynamic details of the wing. Airfoil is a fundamental part of every wing. Wing of paraglider is inflated by moving air. Purpose of this paper is to describe the influence of this inflation on the aerodynamic characteristics of the airfoil.

Key-words: CFD; airfoil; paraglider; aerodynamic coefficient

1. Paraglider airfoils - introduction

Typical paraglider wing can be seen in figure 1. It consist of the wing, made from a textile fabric from the suspension lines and the harness with pilot. Advantage of fabric wing is that the wing can be packed to backpack but during the flight the wing has to be filled with air.



Fig. 1. Typical paraglider wing.

When the inner pressure is higher than the pressure surrounding the wing, the wing is inflated and stable. The higher the inner pressure is the more sta-

ble shape the paraglider has. Wing is filled by air through the wing intakes called cell openings. Detail of them can be seen in figure 2.



Fig. 2. Detail of the paraglider intakes.

Dimension of the intakes can vary from 2 to 10% of the airfoil cord. Smaller ones are used for high-performance paraglider wings. Those wings has lower "passive" safety, they need pilots capable to control the paraglider more precisely especially in the turbulent flying condition to achieve stable flight.

As we can see the paraglider wing is affected by the inflation. The skin of the wing is bulging and many wrinkles can be seen near seams. The effects of the intake and the bulging on the aerodynamic characteristics are the aims of presented analysis. The results from this analysis can be used as the input for performance analysis of whole paraglider wing with proper method, for example [1].

2. CFD model

CFD software Ansys Fluent was chosen for solution of incompressible RANS equation. The structured hexa meshes were created in the Icem CFD software. First of all the 2D analysis of the non-inflated airfoil with multiple meshes were computed. The dimensions of the rest meshes was set according to this mesh-dependency study. Second step was the analysis of 2D geometry of with the intake and the last step was the 3D analysis of the paraglider cell with bulging and intake. 3D geometry was created according to the methodology created by Pohl [2].

*Kontakt na autora: robertkulhanek@gmail.com

2.1. 2D geometry

The analyzed paraglider airfoil has 18% relative thickness located at 24% of the cord. Maximum chamber of the airfoil is 2% and it is located at 17% of the cord. The length (x-distance) of the intake is 4% and front part of the intake is located at 1% of the cord. It is the typical airfoil used in performance paraglider.

In the figure 3 we can see leading edges of the original rib airfoil (black) and the airfoil from the middle symmetrical plane of the cell (red). Generation of that shape is described in the following chapter.

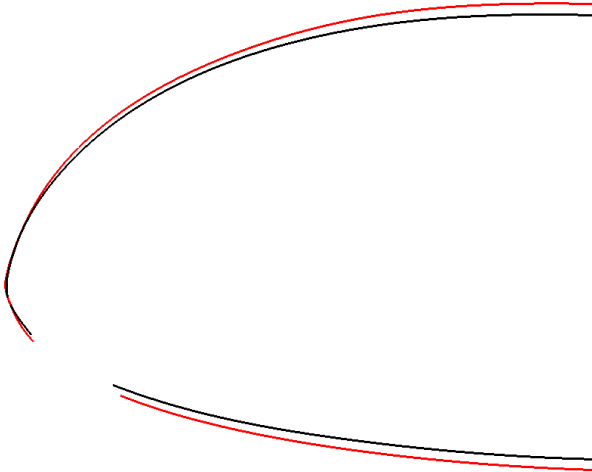


Fig. 3. Comparison of leading edges.

2.2. 3D geometry

3D geometry is based on the generalized relations based on the experimental measurements of multiple parawing. Pohl [2] deduced that the inflated shape of the paraglider cell depends on its aspect ratio (λ_{cell}) and on the lift coefficient.

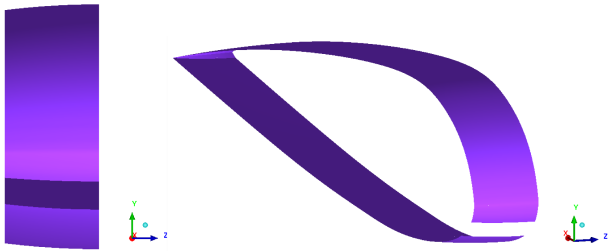


Fig. 4. Detail of 3D model of the symmetrical half part of the cell.

The shape of the upper and lower skin of the inflated cell can be computed as follows:

$$\bar{y} = -\frac{4\bar{U}}{\bar{K}}\bar{Z}^2 + \bar{U} \quad (1)$$

where \bar{Z} is the nondimensional lateral coordinate of the cell

$$\bar{Z} \in \left\langle -\frac{\bar{K}}{2}; \frac{\bar{K}}{2} \right\rangle \quad (2)$$

\bar{K} is the relative contraction of the cell and can be computed according the following relation. The constants C_1 and C_2 correct the equation on the effect

of different thickness and different pressure condition surrounding the airfoil.

$$C_1 = \frac{17}{\bar{t}} \quad (3)$$

$$C_2 = \frac{0.11C_L}{C_{pm}\lambda_{cell}}C_1 \quad (4)$$

$$\bar{K} = 1 - 0.3759\frac{1}{\lambda_{cell}}C_1 - C_2 \quad (5)$$

and \bar{U} is the maximum displacement of the cell in its middle dimension.

$$\bar{U} = \left(0.1735\frac{1}{\lambda_{cell}^2} + 0.1476\frac{1}{\lambda_{cell}} \right) C_3 \quad (6)$$

The constant C_3 is the ration of the relative contraction \bar{K} where the constants C_1 and C_2 are neglected and the \bar{K} computed exactly from the equation 5.

The constant C_2 needs the solution dependent values, namely C_L and C_{pm} . Those values was estimated from the 2D solution of the aifoil with the intake.

2.3. Boundary condition and solver settings

The Reynolds number of all simulated cases was equal to 2×10^6 . Velocity inlet and pressure outlet boundary condition was used on proper boundaries and no slip condition was used on walls. Flow was modelled as incompressible using RANS equations closed by Spalart-Allmaras turbulence model. For fully turbulent condition the modified turbulent viscosity inlet boundary condition was set according to paper [3]. 3D geometry was modelled as symmetrical half with symmetrical boundary condition at the half-plane. The symmetrical boundary condition was also used at the other side of the 3D paraglider cell. This symmetry is assumption of the model. For all of the variables the second order discretization scheme was used. Computation was performed with ANSYS Fluent CFD solver.

2.4. Computational mesh

Far-field was chosen far enough to preserve effect of the boundary condition to the results. Inlet boundary was 11 chord far and outlet was placed 15 chord downstream. The mesh was constructed as hexastructured in ICEM CFD.

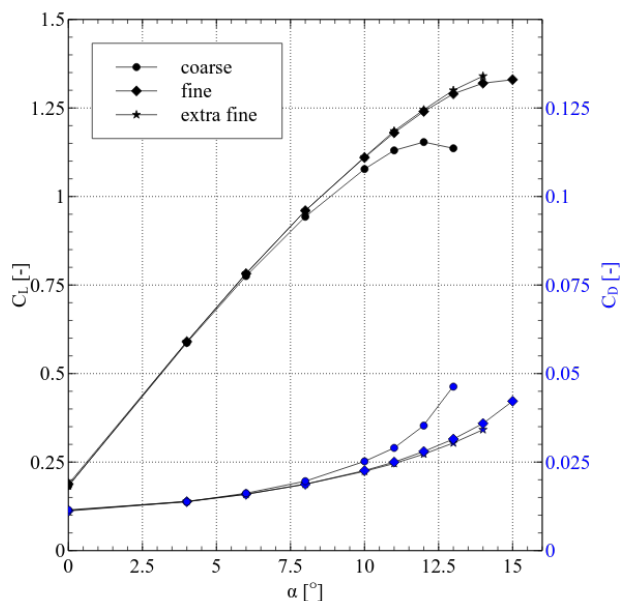


Fig. 5. Results from multiple meshes.

As we can see in the Fig. 5 the results between fine and extra fine meshes are almost identical. The rest of meshes was created with the same spacing as has the fine mesh. All of the meshes was created with condition for employing the enhanced wall treatment ($y^+ < 1$).

Table 1. Dimensions and sizes of used meshes.

Mesh	Number of elements	Nodes around airfoil
coarse	16428	98
fine	31048	165
extra fine	147738	540

3. Results

The results from the computation of the theoretical airfoil placed in the rib of the paraglider are compared with the same airfoil with intake and with the aerodynamic characteristics of the 3D cell and finally with the 2D airfoil from the symmetrical plane of the 3D cell.

3D computation was very time expensive. In fact for each computed point was necessary to create new geometry and computational mesh. It was decided to perform the computation only in region of the operating angles of attack. Calculation of the 2D airfoil from the symmetry plane ("middle" in Fig. 6) was performed also in this limited analysis region. Results can be seen in Fig. 6.

3.1. Effect of the intake

We can observe that the effect of the intake on the lift characteristics is almost negligible. Inlet has effect only in the small region near the stall. Drag characteristics are not influenced in operation range of the airfoil. Moment characteristics are not influenced at all. In the figure 7 we can observe pressure coefficient in the region close to leading edge. When the stag-

nation point is in the place of the intake the integral aerodynamic coefficients are almost identical.

3.2. Effect of the 3D shape

Spatial geometry is solution dependent, only limited number of computations were performed. 3D shape increase C_D if factor of 0.002. Slope of the lift curve is decreased. Derivative $\frac{\partial C_m}{\partial \alpha}$ was not changed but absolute value of C_m was decreased.

2D airfoil from the symmetry plane has the same C_m as 3D cell airfoil. In fact this airfoil is thicker and has relative thicker trailing edge. This explains the pessimistic C_D and $\frac{\partial C_L}{\partial \alpha}$ values. But in general, the results of this airfoil geometry is much more closer to 3D cell results with less computational time. All of the airfoils with intake has the same internal pressure at same angle of attack.

4. Conclusion

Typical paraglider airfoil was analyzed and effect of intake and bulging was quantified. From presented analysis we can deduce that we can simplify full 3D airfoil with the one from symmetry plane of the cell. Analysis on internal pressure can be performed on the rib airfoil. Numerical simulation show us that flow inside the paraglider cell is steady.

Acknowledgement

This work was realized thanks to the grant of ministry of education SGS16/070/OHK2/1T/12.

Nomenclature

c	airfoil cord (m)
b	cell widths (m)
λ_{cell}	aspect ratio of the cell $\frac{c}{b}$ (-)
\bar{U}	maximum normal displacement, relative to cell width b (-)
\bar{K}	relative contraction of the cell $\frac{Z}{b}$ (-)
\bar{Z}	relative lateral coordinate of the cell (-)
C	coefficient of: (-)
p	pressure (-)
L	lift (-)
D	drag (-)
m	moment to 0.25 point (-)
α	angle of attack ($^\circ$)

References

- [1] R. Kulhánek. *Aerodynamika zakřivených křídel*. VZLÚ a.s. - Výzkumný a zkušební letecký ústav. Available at: <http://www.vzlu.cz/cs/transfer-26-2015-s987.pdf> (visited on 02/09/2016).
- [2] L. Pohl. *Aerodynamický výzkum leteckých profilů pro padákové kluzáky*. 2011.
- [3] Philippe R. Spalart Steven R. Allmaras Forrester T. Johnson. *Modifications and Clarifications for the Implementation of the Spalart-Allmaras Turbulence Model*. ICCFD-1902.

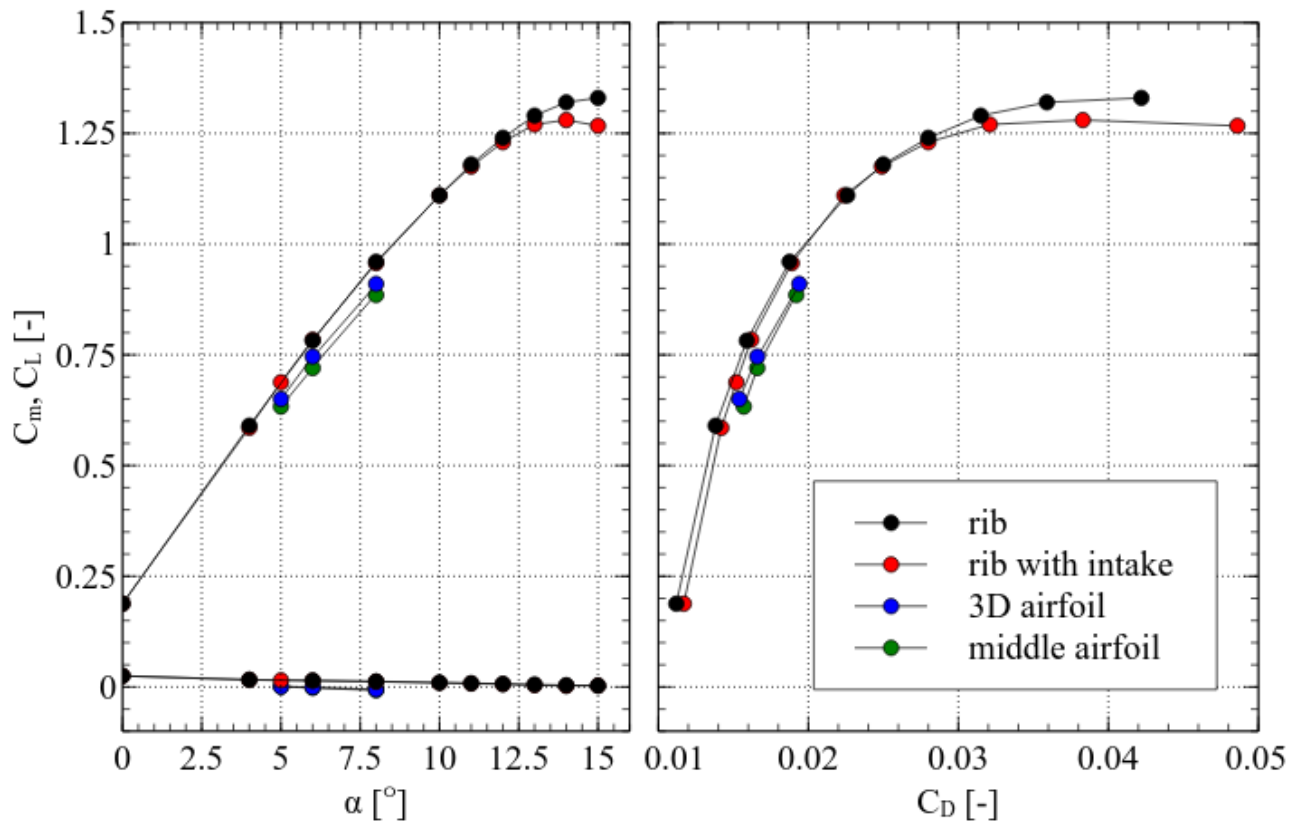


Fig. 6. Comparison of computed results.

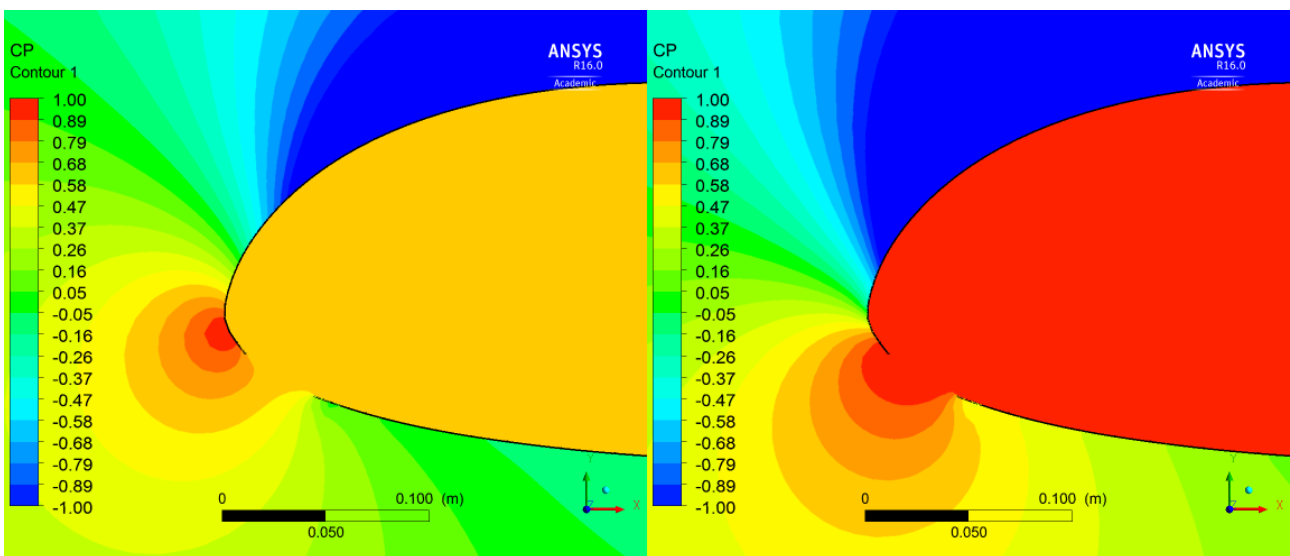


Fig. 7. C_p of rib airfoil with intake. Left 4° and right 8° angle of attack